Robotica (2011) volume 29, pp. 23–34. © Cambridge University Press 2011
doi:10.1017/S0263574710000676

A low-cost approach for self-calibration of climbing robots

Mahmoud Tavakoli*, Lino Marques and Aníbal T. de Almeida

Department of Electrical and Computer Engineering, Institute for Systems and Robotics, University of Coimbra, Coimbra 3030-290, Portugal. E-mails: {mahmoud,lino,adealmeida}@isr.uc.pt

(Received in Final Form: October 22, 2010)

SUMMARY

High accuracy is usually difficult to obtain with a robotic arm installed on a mobile base, since the errors of the base are transferred to the manipulator. This paper proposes a method to address this problem through integration of a self-calibration algorithm and low-cost sensors. The self-calibration algorithm might be repeated several times during execution of a mission by the robot and is only based on the internal sensors of the robot, meaning that external observers or reference point transceivers (e.g., ultrasonic transceivers) are not used. The proposed self-calibration system was implemented on a pole climbing robot and effectively improved the positioning accuracy of the climbing arm.

KEYWORDS: Climbing Robots; Mobile Arms; Self Calibration; Accelerometers; Gripper; Positioning Error.

1. Introduction

Service robots have a vast variety of applications comprising housekeeping, agriculture, inspection, construction, etc. Many service robots are composed of a mobile base, a robotic arm and an end effector connected to the manipulator for performing specified operations. In many cases the manipulator is intended to perform fine manipulation and, therefore, high positioning accuracy is necessary. Some of the service robots comprise a large manipulator and it is well known that larger manipulators contain bigger positioning errors. Some methods and tools have been used to compensate such errors addressing the fine manipulation problem of industrial arms (e.g., application of strain gauges in flexible arms or theodolites for pose estimation)[6,11]. However, the problem of accurate positioning of the manipulator deals with another error source, which is not the case for fixed industrial manipulators. The mobility of the base merges an error to the base of the robot and since the manipulator trajectory is calculated relative to the base, any error in the base of the robot is magnified through multiplication by the length of the links and is transferred to the manipulator. Consequently, fine manipulation involves more problems to be addressed if the base of the arm is mobile.

Climbing robots are a branch of service robots mainly intended to perform cleaning, maintenance and inspection missions on elevated structures. Some of these applications, e.g., welding on pipelines require fine manipulation. To perform such tasks, one may equip the climbing robot with an additional accurate manipulator. But in many cases, to avoid complexity of the system, a single structure is designated for both climbing and manipulation[3,19,22].

Furthermore, in industrial arms with a fixed base, the manipulator may calibrate itself through finding a fixed zero reference on the base, while in climbing robots the base is not fixed. Therefore this problem should be addressed by an alternative method. This paper proposes a self-calibration method to address this problem for a 6-degree of freedom (DOF) arm installed on a mobile base. The so-called self-x systems should be able to dynamically adapt to changes in requirements to automatically detect and neutralize component failures and to continuously optimize themselves for better performance.

It is important to mention the difference between autonomous calibration and self-calibration. Self-calibration methods require only information gathered by a robot's internal sensors, while autonomous calibration methods may utilize external devices, mechanisms, sensors, or reference points. For instance, Rauf and Ryu[18] introduced a fully autonomous calibration of parallel manipulators by imposing position constraint. They locked the manipulator so that its translational DOFs are removed. Thus, six actuator sensors are used to measure only three DOFs. Thus, to lock the mechanism they require an external device. Many autonomous calibration methods suggest using laser displacement sensors to measure the distance from several fixed points in the workspace to the robot's endpoint[9]. Still, the fixed points are used as external reference points. Calibration of a manipulator using external fixed points can only be called as "self-calibration" if the external references are not engineered.

For instance, considering a mobile robot, it may measure the distance from the ground surface or walls if the ground is a plain surface without any designated symbol on it. If the robot uses any engineered shape or landmark on the wall or ground for calibration purposes, it can not be considered as "self-calibration". Khalil and Besnard reported the development a method for self-calibration of Stewart-Gough parallel robots without extra sensors[10]. Yet they use an extra mechanical locking linkage, and thus their method is not completely "self-calibration."

An example of a self-calibration method can be seen in ref. [5]. Per Henrik *et al.* developed NIMS-PL, a 2-DOF cable-driven robot with self-calibration capability. As stated by the authors, methods to accurately calibrate these systems often require data acquisition from external

* Corresponding author. E-mail: mahmood.tavakoli@gmail.com

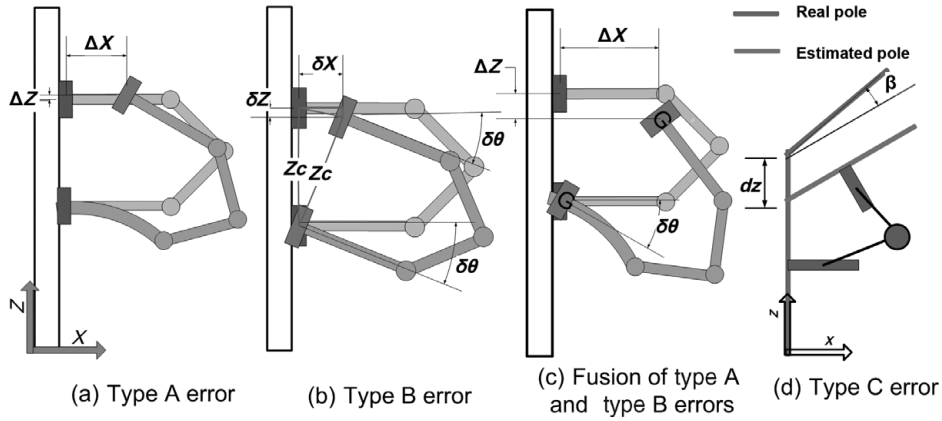

Fig. 1. An exaggerated representation of error source for an arm with a mobile base. (a) Error due to the deflection of arm links. (type A). (b) Errors due to the mobility of the base (type B). (c) Fusion of both errors. δX, δZ, and $\delta\theta$ are deviations from the desired pose. (d) Type C error: errors related with the inaccurate data/estimation of the angle of a bent section, or the distance from the gripper to the structure.

calibration-specific sensors, such as laser displacement sensors. As dependence to an external sensor is not desirable for an autonomous system, they developed two self-calibration methods that leverage the robot's actuation redundancy. In their method the variation in cable tension is used in order to determine the end-effector location. A "self-calibration" method should have the following characteristics:

1. Increase the system accuracy through repeated autonomous calibration.
2. Distinguish the appropriate time to carry out the calibration and perform the calibration autonomously.
3. Avoid using any external observer, engineered shape or designated symbol, or external mechanisms, and devices.

In this paper, we show how the positioning accuracy of a robotic arm with a mobile base can be improved by a repeated self-calibration algorithm. In this method by integration of inertial sensors, infrared range sensors, and a self-calibration algorithm, a low-cost solution is proposed. The proposed solution is totally embedded into the system. The robot calibrates itself without requiring any external observer. Being independent of an external system is a key factor in self-x systems.

During the last two decades many climbing robots have been developed for different applications and with different levels of mobility. Some of them can only climb a straight line on a flat surface[16]. Some others can move on both directions of a flat vertical plane and take any orientation on the plane[17]. The most complicated group of climbing robots are those that can traverse across planes[8]. Another complex branch of climbing robots are pole climbing robots, which can climb over 3D tubular structures, e.g., pipelines, can pass bent sections, and overcome T-junctions. The main focus of this paper is the later group. To be able to traverse across planes or to pass bent sections, the climbing robot is usually composed of at least two grippers or adhesion zones, which are connected together through a multi-DOF climbing structure[1,3,13,19,23]. These robots may have an additional arm to perform the desired inspection or maintenance across the pole, or may use the climbing mechanism arm for this purpose.

Section 2 of this paper describes extensively the problem of fine manipulation in climbing robots. Section 3 describes the formulation of the problem and the proposed solution. Section 4 describes the implementation of the proposed method on the 3DCLIMBER and presents the results extensively. The preliminary results of these experiments were published in ref. [20].

2. Problem Statement

As has been stated earlier, this paper focuses on climbing robots, which can traverse across different working planes. Such robots are usually composed of at least two grippers or adhesion zones connected through a multi-DOF arm. When the robot intends to traverse across two planes, the multi-DOF arm should place the adhesion zones on the desired plane. The arm might be an articulated serial arm[3], a parallel or Stewart mechanism[1], or a hybrid mechanism[21]. In all cases, the manipulator of the arm contains positioning errors. Error sources, which are the main cause of the inaccuracy in the positioning system of a climbing robot, can be divided into the following three main groups:

- *General error sources of industrial robotic arms* (*type A errors*)
  High accuracy is generally difficult to obtain in large manipulators capable of producing high forces due to system elastic and geometric distortions[14]. Due to some sources of errors, namely tolerance on gears, coupling errors, deflection of the links, etc., the manipulator has positioning errors. This is a general problem of the robotic arms, which has been discussed in the literature. For instance, the control problem of flexible link robotic manipulators has been studied in the last two decades[6]. Some control strategies (i.e., fuzzy and adaptive control) have been proposed[11]. To measure the amount of the deflection, two strain gauges are usually stuck onto the arm[11]. Most manipulator calibration techniques require expensive and/or complicated pose measuring devices, such as theodolites[15]. For simplicity of referencing, this type of error is called the type A error (Fig. 1(a)).

https://doi.org/10.1017/S0263574710000676 Published online by Cambridge University Press

- *Error sources due to mobility of the arm base* (*type B errors*)
  In industrial robotic arms, the base of the robot is usually fixed to a certain point. Multi-DOF climbing robots usually consist of an arm and two or more gripping mechanisms. During climbing, the gripper, which is fixed, is called the "base" and the other gripper, which is moving, is called the "manipulator." The base and the manipulator change their role in each step and as the manipulator movements are programmed relative to the base, errors in pose of the base will cause errors in pose of the manipulator (Fig. 1(b)). For simplicity of referencing, this type of error is called the type B error.
- *Error sources because of the inaccurate estimation of bent angle* (*type C errors*)
  Climbing robots may traverse between different working planes. These working planes constitute an angle relative to each other. To traverse between these planes, the path planner should receive this angle as input. This angle might be determined by several methods. It might be provided to the robot by the operator when *a priori* knowledge of the environment or even a rough estimation of the world is available. In other cases, vision or other world modeling techniques might be used for modeling the environment. In any of these cases, the pre-determined value of this angle may contain errors. Such errors affect the path that is planned by the path planner. We call this the type C error (Fig. 1(d)). Furthermore, before traversing between working planes, the robot should know its distance to the working plane. Also, the position where the working plane starts might be a source of error, which is shown by dz in Fig. 1(d)).

Figure 1 (a) demonstrates the error due to the deflection of the arm links (type A error). Figure 1(b) represents how the deviation angle of the robot's base around the "Y" axis due to the mobility of the arm (type B error) causes a positioning error on manipulator. Figure 1(c) demonstrates an exaggerated representation of both errors fused and Fig. 1(d), shows type C errors.

Figure 2 shows another form of type B error. In the system shown in Fig. 2, the climbing robot is composed of two adhesion zones that pose an embedded vacuum system and a multi-DOF mechanism. Mobility of the adhesion zone causes an error around the "Y" axis (Fig. 2, left) or around the "X" axis (Fig. 2, right), which is transferred to the upper unit.

In step-by-step-based climbing robots, this error is accumulative and the total deviation from the desired position and angle becomes increasingly larger after each step. In the case of climbing robots with seizing grippers, owing to the accumulated error after a few steps, a gripper may not be able to grasp the structure because of the excessive positioning error, and therefore the operator has to stop the operation, manually calibrate the robot, and then resume the operation. In the case of adhesive grippers, magnets, or vacuum grippers, this might not be the case and an appropriate design of the gripper with passive joints makes the gripper tolerant to such errors. Even for seizing grippers, integration of compliance to the system through compliant materials, compliant mechanisms, or compliant control increases the tolerance to such errors. Yet being tolerant to such errors means that the gripper can attach to the structure, but still the type B error exists, since the gripper is attached in a different unknown pose than what was expected. In this case, necessary sensors should be integrated in order to measure the amount of error on the pose of the gripper and to compensate the type B error generated on the manipulator.

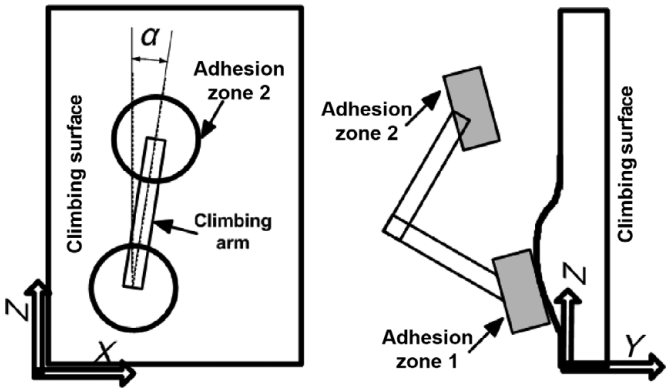

Fig. 2. A robot with two adhesion zone units. Left: α is the error around the "Y" axis on the lower adhesion zone unit, which is transferred to the upper unit. Right: Error on adhesion zone 1 due to an uneven area.

For general formulation of the problem, an arm with 6-DOF with a mobile base is considered. However, in many cases climbing robots comprise a mechanism with less than 6-DOF[3, 19, 21]. Figure 3 shows a schematics of a 6-DOF articulated arm. If the base has an angular deviation from its desired pose, it makes an error on the pose of the manipulator (in all six translational and rotational components).

A robotic arm, which is intended for manipulation across the climbing surface, might be an independent arm installed on a climbing robot, or a part of the climbing mechanism itself. The objective of this research is to develop a self-calibrating method to reduce the positioning error of the arm every time it passes a predefined allowed error on each component of the pose so that the positioning accuracy of the manipulator be independent from the errors of its base. The manipulator should be able to move in a predefined pattern, namely a line or a circle (usually required for welding robots), even if the robot's base (the adhesion zone) is not well-positioned.

An important aspect of the problem that should be considered is that, due to mobility of the system, some solutions, which can be used for fixed systems, are not applicable in a mobile system. In many applications, the absolute pose of each link of an articulated arm can be obtained with different strategies, namely by triangulation or by trilateration to a fixed reference system. In both cases, a reference base station is required and should be calibrated before starting the robot operation. For instance, this might be done by installing infrared LEDs on different locations of the robot and locate their location by an external observer (infrared detector), or by using ultrasonic transceivers. However, this might not be a practical solution for outdoor industrial applications, as the installation and calibration of the observer is a time-consuming task requiring an expert. Since many climbing robots are designated to operate in

https://doi.org/10.1017/S0263574710000676 Published online by Cambridge University Press

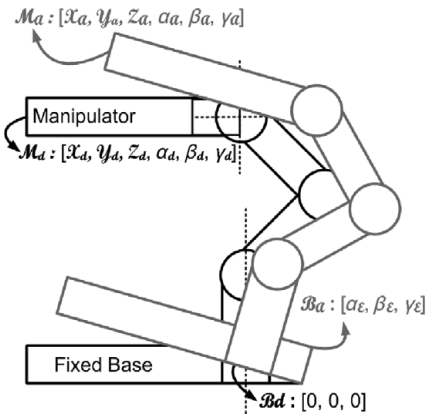

Fig. 3. The angular deviation on the robot base causes an error on the pose of the manipulator. $[\alpha,\ \beta,\ \gamma]$ represent the angular deviation of the base, and M_a and M_d represent the actual and the desired positions of the manipulator.

multiple structures and places, a solution, embedded into the robot and independent from the external references or devices, is highly preferred.

3. The Proposed Method

In order to describe the proposed self-calibration method, first the sensors, which are necessary for achievement of the method, are delineated and then the calibration algorithms are described.

3.1. Variables to be measured

In order to implement the calibration system, some variables in task space should be measured. The value of those variables can not be estimated accurately solely by joint sensors (e.g., encoders) and additional sensors should be integrated. The sensor redundancy for estimation of these variables is explained. The sensors described here are designated for a 6-DOF manipulator with a mobile base; however, in many cases some of these can be neglected (e.g., when the arm has less than 6-DOF or when the error in one of the components is very small). As shown in Fig. 4, an inertial measuring system (IMS) and a range-finder should be installed on each gripping unit. Also, an infrared emitter and detector are necessary.

The IMS can measure the absolute angle of each gripping module and report the angular deviation from the desired pose independent from the climbing surface inclination. This can be done by calculating the changes on the effect of the gravity acceleration on the output of the accelerometer axes as well as the output of the 3D compass. As the base and the manipulator of a climbing robot change their role at each step, an IMS for each of them is necessary. In many cases the application of inertial unit is not necessary and a 3-axis accelerometer is sufficient. A low-cost range sensor should be installed on each gripping unit to measure the distance between the gripper and the climbing surface/structure. The infrared emitter and detector will be used to calibrate Y and Z components of the manipulator pose. The role of these

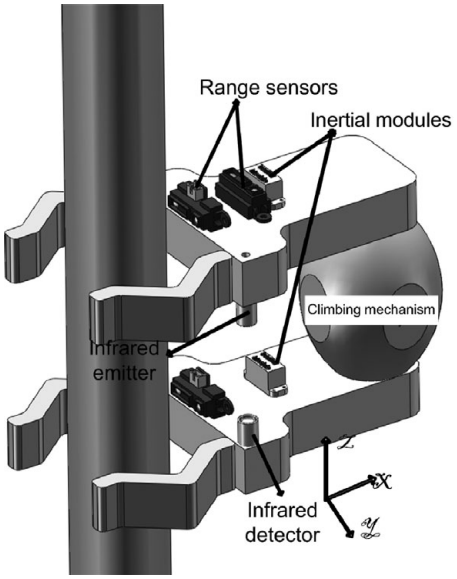

Fig. 4. Necessary sensors for the self-calibrating algorithm of the climbing robots.

sensors will be explained more extensively along with the description of the calibration algorithm.

3.2. Necessity for range sensors

By using an IMS, the distance estimation can be obtained by double integration of acceleration with time and thus the distance paved by the robot's gripping units can be estimated by the integrated IMS units. Therefore, the necessity for existence of range-finding sensors and infrared emitter and detector can be discussed. While range-finding sensors take advantage of absolute distance measurement, the IMS estimation from distance is relative. Hugh *et al.*[12] discussed the application and accuracy of accelerometers in mobile robots. As an example, they moved an accelerometer for a distance of 120 cm with an acceleration of 8 m/s^2. Using a Kalman filter, the final distance error accumulated was 1.08 cm (less than 1%). Many factors effect the accuracy of accelerometers, including temperature, acceleration, sensitivity, etc. Despite all these factors, the decision about the necessity of range sensors in the system depends on the accuracy that the system requires and the distance that it should pave on the structure. As the position error is accumulative, longer distances cause bigger errors. Furthermore, if the robot intends to move in unknown environments, it is not anymore enough to obtain information relative to the initial position. The robot needs to know its distance toward the environment. This distance can be measured only with sensors that obtain information from the environment, e.g., stereo-cameras, laser range-finders, or range sensors (ultrasonic or infrared). The simplest and the cheapest ones are the infrared range sensors; that is why we used the same in this study.

3.3. Quantity of range sensors

The quantity of the necessary range sensors for the execution of the self-calibration algorithm depends on the complexity of the climbing structure and also on the robot's DOF

https://doi.org/10.1017/S0263574710000676 Published online by Cambridge University Press

number. A robot, which is intended to climb from a plane without traversing between different planes, may only use one range sensor on each adhesion zone to measure the distance between the gripper and the climbing plane. If the robot can traverse directly to any plane (for instance, from XY to XZ and YZ), which is the case for 6-DOF climbing robots[4], three range-finders should be installed on each adhesion zone. The reason is that since the robot may traverse to any plane, the distance between the gripper and all those planes should be known. In this case, the manipulator should locate itself relative to those planes in all three translational directions (X, Y, and Z). In some cases, the robot has a 4-DOF climbing mechanism[2,19,22] and to traverse to other planes it may pass through mediatory planes. In this case two range-finders are adequate because the robot only uses two traverse directions. A 6-DOF mechanism may be equipped with only one range sensor. In this way the measurements for all three planes can be done by changing the orientation of the manipulator. However, this method increases the time and energy costs, and furthermore all poses might not be possible for the manipulator because of the possible lack of space in an unknown environment or the manipulator's limitations. In an alternative approach, low-cost range sensors with different orientations can be installed at different locations of the manipulator. The advantage of this approach is that these sensors can rapidly gather the necessary data from the environment.

3.4. Error estimation

Considering a 6-DOF mechanism, and apart from any type of robotic structure and actuator that have been used:

The input of the joints are considered as $[\theta_1, \theta_2, \theta_3, \theta_4, \theta_5, \theta_6]$ (Fig. 3) and the manipulator pose is shown as $[X, Y, Z, \alpha, \beta, \gamma]$. Therefore,

$$[\theta_1, \theta_2, \theta_3, \theta_4, \theta_5, \theta_6] \xrightarrow{\textit{Direct Kinematics}} [X, Y, Z, \alpha, \beta, \gamma], \tag{1}$$

$$\overrightarrow{M_a} = \overrightarrow{M_d} + \overrightarrow{\varepsilon_b} + \overrightarrow{\varepsilon_o},$$
$$\overrightarrow{\varepsilon_o} = [\varepsilon_x, \varepsilon_y, \varepsilon_z, \varepsilon_\alpha, \varepsilon_\beta, \varepsilon_\gamma],$$

where
$M_a : [X_a, Y_a, Z_a, \alpha_a, \beta_a, \gamma_a]$: the actual pose of the manipulator,
$M_d : [X_d, Y_d, Z_d, \alpha_d, \beta_d, \gamma_d]$: the desired pose of the manipulator,
ε_b: the error on the pose of the manipulator initiated from the angular deviation of the base (type B error),
ε_o: the error on the pose of the manipulator initiated from the other factors (type A error).

To calculate ε_b, the 6-DOF manipulator can be remodeled as a redundant mechanism with nine active actuators, assuming that the 6-DOF mechanism is installed on a 3-DOF base. The base is considered as a 3R mechanism, which rotates the manipulator around all three axes ("X," "Y," and "Z"). The angular deviation of the base can be calculated as the difference between the desired inclination of the base relative to a fixed coordinate and the actual inclination of the base reported by the inertial measuring system and is shown as $B_a = [\alpha_\varepsilon, \beta_\varepsilon, \gamma_\varepsilon]$. Then the error on the pose of the manipulator initiated from the angular deviation of the base (ε_b) can be calculated by multiplying the transform function of the considered 3-DOF base by the desired position of the base:

$$\overrightarrow{\varepsilon_b} = T(\alpha_\varepsilon, \beta_\varepsilon, \gamma_\varepsilon).[X_d, Y_d, Z_d, \alpha_d, \beta_d, \gamma_d],$$

where $T(\alpha_\varepsilon, \beta_\varepsilon, \gamma_\varepsilon)$ is the transform function of the 3-DOF base, and $T(X_d, Y_d, Z_d, \alpha_d, \beta_d, \gamma_d)$ is the transform function of the 6-DOF mechanism, which is normally shown as ${}^0T_6$. If we present ${}^0T_6$ of the desired pose as

$${}^0T_6(P_d) = \begin{pmatrix} r_{11} & r_{12} & r_{13} & X_d \\ r_{21} & r_{22} & r_{23} & Y_d \\ r_{31} & r_{32} & r_{33} & Z_d \\ 0 & 0 & 0 & 1 \end{pmatrix},$$

then applying the Denavit Hartenberg convention[7], $T(\alpha_\varepsilon, \beta_\varepsilon, \gamma_\varepsilon)$ can be calculated as:

$${}^0T_3 = \begin{pmatrix} C(\gamma_\varepsilon)C(\beta_\varepsilon)C(\alpha_\varepsilon) + S(\gamma_\varepsilon)S(\alpha_\varepsilon) & -C(\gamma_\varepsilon)C(\beta_\varepsilon)S(\alpha_\varepsilon) + C(\alpha_\varepsilon)S(\gamma_\varepsilon) & 0 & 0 \\ S(\gamma_\varepsilon)C(\beta_\varepsilon)C(\alpha_\varepsilon) - C(\gamma_\varepsilon)S(\alpha_\varepsilon) & -S(\gamma_\varepsilon)C(\beta_\varepsilon)S(\alpha_\varepsilon) - C(\alpha_\varepsilon)C(\gamma_\varepsilon) & 0 & 0 \\ S(\beta_\varepsilon)C(\alpha_\varepsilon) & -S(\beta_\varepsilon)S(\alpha_\varepsilon) & 0 & 0 \\ 0 & 0 & 0 & 1 \end{pmatrix}.$$

Considering:

$$\overrightarrow{\varepsilon_b} = [\varepsilon_{bx}, \varepsilon_{by}, \varepsilon_{bz}, \varepsilon_{b\alpha}, \varepsilon_{b\beta}, \varepsilon_{b\gamma}],$$

the error components can be calculated by multiplying ${}^0T_3.{}^0T_6(P_d)$. Thus,

$$\begin{aligned} \varepsilon_{bx} &= X_d(C(\gamma_\varepsilon)C(\beta_\varepsilon)C(\alpha_\varepsilon) + S(\gamma_\varepsilon)S(\alpha_\varepsilon)) \\ &\quad + Y_d(-C(\gamma_\varepsilon)C(\beta_\varepsilon)S(\alpha_\varepsilon) + C(\alpha_\varepsilon)S(\gamma_\varepsilon)), \\ \varepsilon_{by} &= X_d(S(\gamma_\varepsilon)C(\beta_\varepsilon)C(\alpha_\varepsilon) - C(\gamma_\varepsilon)S(\alpha_\varepsilon)) \\ &\quad + Y_d(-S(\gamma_\varepsilon)C(\beta_\varepsilon)S(\alpha_\varepsilon) - C(\alpha_\varepsilon)C(\gamma_\varepsilon)), \\ \varepsilon_{bz} &= X_d(S(\beta_\varepsilon)C(\alpha_\varepsilon)) + Y_d(-S(\beta_\varepsilon)S(\alpha_\varepsilon)). \end{aligned}$$

Also the rotational components of $\overrightarrow{\varepsilon_b}$ can be obtained from the ${}^0T_3.{}^0T_6(P_d)$ vector.

On the other hand, to calculate ε_o, the inertial sensor and the range finder installed on the manipulator as well as the infrared transmitter and detector are used. We will describe later how all six components of the manipulator pose can be measured by the mentioned sensors. ε_o can be measured simultaneously with ε_b, or can be measured after compensation of the base errors. The latter method is slower, as the system should perform the measurement in two sequential steps, but it is more accurate because, after compensation of ε_b, the manipulator is positioned more accurately and thus the measurements of the infrared and range sensors are more accurate. If the latter method

https://doi.org/10.1017/S0263574710000676 Published online by Cambridge University Press

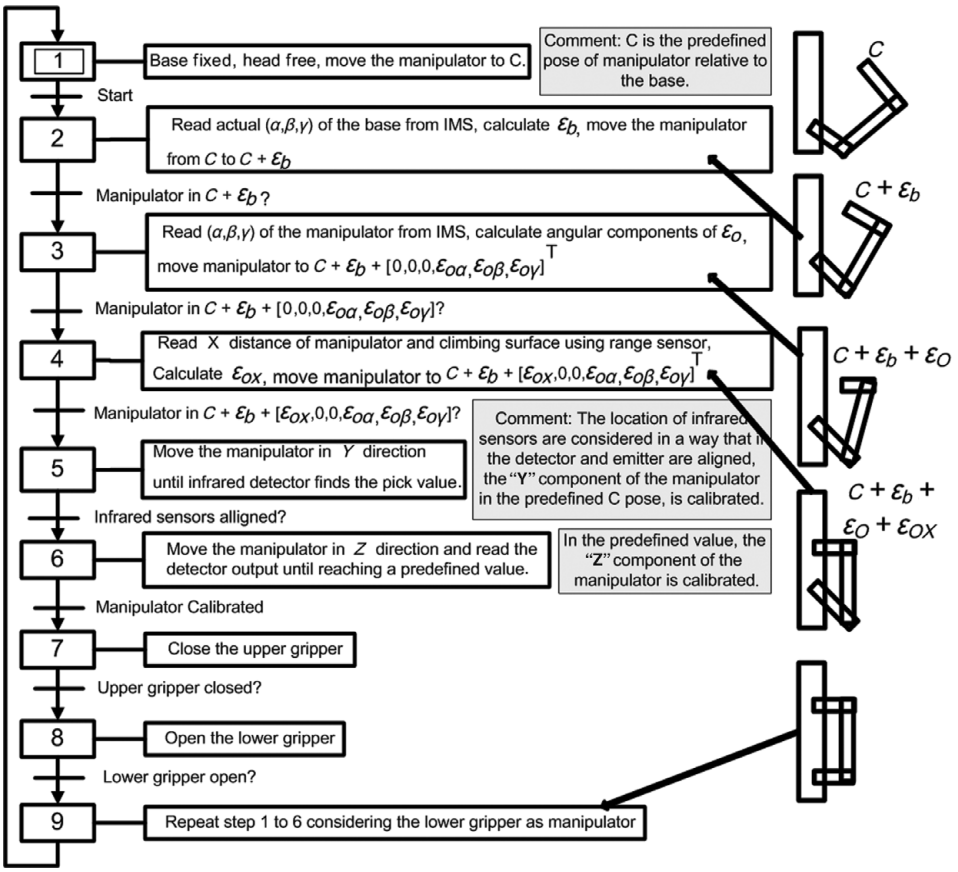

Fig. 5. A simplified Grafcet representation of the calibration algorithm.

(sequential measurement and calibration) is applied, ε_o can be calculated as

$$\begin{aligned}\overrightarrow{\varepsilon_o} &= [\varepsilon_{ox}, \varepsilon_{oy}, \varepsilon_{oz}, \varepsilon_{o\alpha}, \varepsilon_{o\beta}, \varepsilon_{o\gamma}],\\ &= [X_d - X_m, Y_d - Y_m, Z_d - Z_m, \alpha_d - \alpha_m, \beta_d - \beta_m,\\ &\quad \times \gamma_d - \gamma_m],\end{aligned}$$

where ε_{ox} is the part of the error on x-axis, which is initiated from all error sources except the mobility of the base, X_d is the desired value for the "X" component of the manipulator, and X_m is the measured "X."

The inertial module measures the angular components of the manipulator pose relative to a fixed coordinate system, the range sensor measures the distance between the manipulator and the climbing surface in the X direction, and the infrared transmitter and detector calibrate the system in the Y direction and measures the distance between the base and the manipulator in the Z direction.

3.5. The calibration method

The inertial sensors and range-finders measure the pose components of the robot's manipulator and base continuously, but if the error in one of the components passes a predefined value, the robot should recalibrate itself. Here, the sequential measurement and calibration (and not the simultaneous) is described. To describe the calibration method, we assume that the robot has two grippers and at the time the error is reported, the lower gripper is the base and the upper gripper is the manipulator of the robot. Figure 5 shows the simplified Grafcet representation of the calibration algorithm. When one of the components of the manipulator pose passes its allowed error value, the self-calibration algorithm is applied. In the first step of the algorithm, the manipulator should move to a predefined pose (C) and then ε_b is calculated based on the measurements of the inertial unit installed on the base of the robot. After compensation of ε_b (type B error), the angular components of ε_o are measured by the IMS and then compensated. This assures that the calibration of the angular components of the manipulator's pose is necessary before application of the range sensor, because if the range sensor is not pointed perpendicular to the surface, it would not report the correct value. The range sensor on the manipulator is then utilized in order to measure and calibrate the manipulator in the X direction. Subsequently, the manipulator moves in the Y direction until the infrared sensors report the pick value. The infrared sensors should be installed in such a way that if the detector and emitter are aligned, the "Y" component of the manipulator in the predefined "C" pose is calibrated. Afterward, the manipulator moves in the Z direction and based on the received value from the infrared detector, the "Z" component of the manipulator is calibrated. In this step, the upper gripper is calibrated and can grasp the structure. Then the lower gripper should release the structure and get calibrated similar to the upper gripper.

A question may arise that while the manipulator can be calibrated using only the sensors installed on it, why the ε_b be compensated first? The answer is that in some cases (for instance, in the case study, which will be presented later in

https://doi.org/10.1017/S0263574710000676 Published online by Cambridge University Press

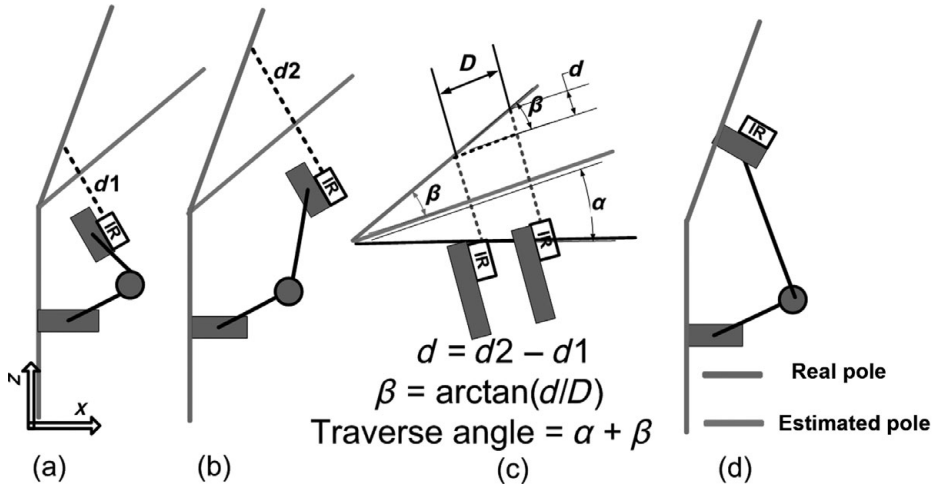

Fig. 6. Demonstration of the algorithm used for addressing the problem of type C errors.

this paper), the type B error is bigger than the type A error. Therefore, if the ε_b is compensated, the positioning error becomes small enough to let us neglect the calibration step for compensation of the type A error and thus eliminates the necessity for the integration of some of the sensors, for instance, the infrared sensors. The second reason is that when system is being calibrated against the type B error, the positioning error of all components of the manipulator pose are compensated simultaneously, but each component of the type A error should be measured and calibrated separately, which is a time-consuming process. Also, it is important to mention that the presented algorithm is a comprehensive algorithm for a 6-DOF mechanism, but depending on the application and also the arm itself, some of the steps can be removed. For instance, it will be shown in the case study in the next section that for a 4-DOF mechanism the utilized sensors and algorithms are highly simplified.

3.6. Extended calibration method for unknown environments – type C errors

To overcome the problems related with the type C error, every time that the robot traverses between different working planes, the manipulator should measure and report the accurate amount of the angle between the planes. This can be done by a simple algorithm using range sensors and the IMS. The calculations related to the proposed algorithm are shown in Fig. 6 and are composed of the following steps. Before traversing to the working plane, one of the range sensors can measure the distance from the pioneer adhesion zone to the working plane.

- Manipulator should be placed accordingly to the estimated bent angle and in a certain distance from the surface. This distance is for avoiding any incident between the manipulator and the climbing surface, in case the estimated angle is bigger than the actual angle (in contrary with what is demonstrated in Fig. 6(a)).
- In this position, the IMS of the manipulator reports the manipulator angle (in Fig. 6, the angle around the "Y" axis is shown as α). Also, the range sensor measures $d1$, the distance between a point in the manipulator and the surface.
- Manipulator moves for a certain distance parallel to the estimated angle (Fig. 6(b)), and measures the distance $d2$. Then the correct angle $(\alpha + \beta)$ is calculated with simple calculations as shown in Fig. 6(c).
- Finally, the path planner calculates the correct adhesion position for the manipulator considering the calculated angle and the manipulator moves to this pose and sticks to the surface (Fig. 6(d)).

4. Case Study

The self-calibration algorithm was tested on 3DCLIMBER, a pole climbing robot for climbing and manipulating across 3D structures with bends and T-junctions[19]. Figure 7 shows the robot passing from a bent section. The robot comprises two gripping modules and a 4-DOF climbing mechanism. Figure 8 shows the model of the climbing structure. To reduce the system weight and complexity, the 4-DOF climbing structure is intended to be used both for climbing and manipulation, and thus the system does not require an additional arm. On the other hand, as the robot is an industrial size climbing robot with a large manipulator, the well-known error sources of large manipulators, in addition to mobility of the base, decrease the positioning accuracy of the robot. After robot development, a preliminary test of the robot proved the lack of precision. Such a problem led to gripping problems because of grippers' inaccurate placing. This was not acceptable because it impairs the autonomous navigation of the robot on the structure. As the error is accumulative, after a few steps the positioning error of the manipulator becomes so big that it makes the gripping action impossible. In this case, the robot cannot continue climbing across the structure until it gets calibrated. In this case the self-calibration algorithm should be executed to help resuming the autonomous navigation of the robot on the structure. Also, the manipulation precision of the robot was very low, containing errors as big as 48 mm in the X direction. To compensate for this error, a simplified version of the self-calibration method (utilizing low-cost accelerometers and range-finders) was applied. In some cases, the problem of bad gripping might be addressed by integration of a compliant

https://doi.org/10.1017/S0263574710000676 Published online by Cambridge University Press

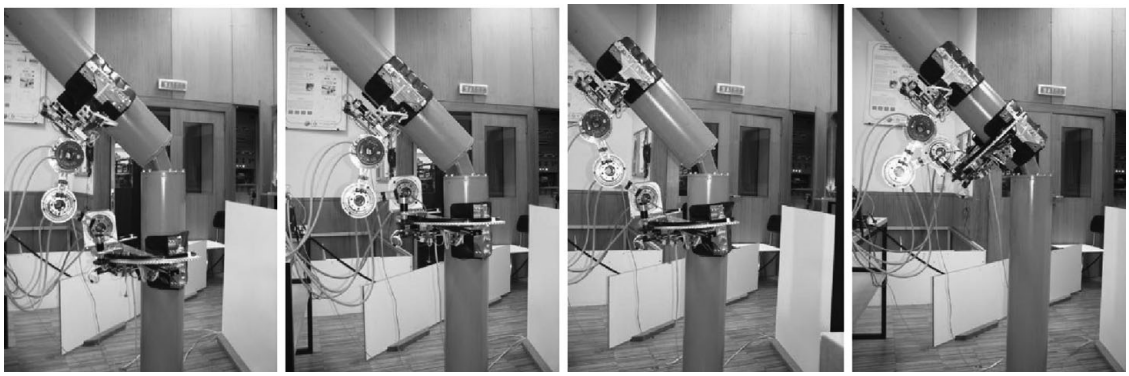

Fig. 7. The 3DCLIMBER robot passing from a bent section.

mechanism on the gripper or by compliance control of the climbing arm motors. But such solutions would not totally address the manipulation accuracy problem.

4.1. Sensors

Compared to a 6-DOF mechanism, the designated 4-DOF mechanism does not include translation along "Y" axis and rotation around "X" axis. Therefore, rather than a complete inertial measuring system, a 2-axes analog accelerometer is utilized. Any change in the angle of each link causes a change on the effect of the gravity acceleration on each axis and thus changes the output voltage of accelerometers. STMicroelectronics ultra compact LIS244AL two-axes analog accelerometer chips were used for this purpose. This chip is integrated in a board and installed on the robot base and manipulator (Fig. 9). The output voltage is read and processed using a PIC microcontroller and the final values are transmitted to the main controller through a Zigbee module. For an effective calibration of the system, a precision of about 0.5° is required. In practice the 3DCLIMBER robot always has vibrations due to spring characteristics of the links.

Vibrations add acceleration to the links, which affect the output value of the accelerometers. The only positive aspect is that these vibrations are of low frequency and mostly under 10 Hz. Therefore, a method which averages sufficient samples acquired at high frequency was applied. If the sampling frequency is adequately greater than the mechanical vibration frequency and if a large enough number of samples are acquired and averaged, then the low-frequency vibrations will be eliminated. In some experiments, we found that the average value of 200 to 400 samples (total time of 2–4 s) acquired at the rate of 100 Hz (10 times larger than the mechanical vibration frequency of the links) is very reliable, as it has good repeatability and can filter the effect of mechanical vibrations. It showed a repeatability precision of 0.07° (4′). To test the repeatability against the mechanical vibrations effect, the plate on which the sensor was installed was manually vibrated with different frequencies and amplitudes similar to what happens with the 3DCLIMBER. The results of these experiments are summarized in Table I. The mean value of the Vout of the "Y" axis did not change by more than 0.1 mV even with the existence of 6 Hz frequency vibrations. The average value in a relatively higher amplitude vibration has only changed by about 1 mV. This provides us with a precision better than 0.3° (20′) even with the existence of relatively high-amplitude vibrations. The developed inclinometers' characteristics are summarized in Table II.

The distance between the pole and the structure is measured using Sharp GP2Y0A21 optical triangulation

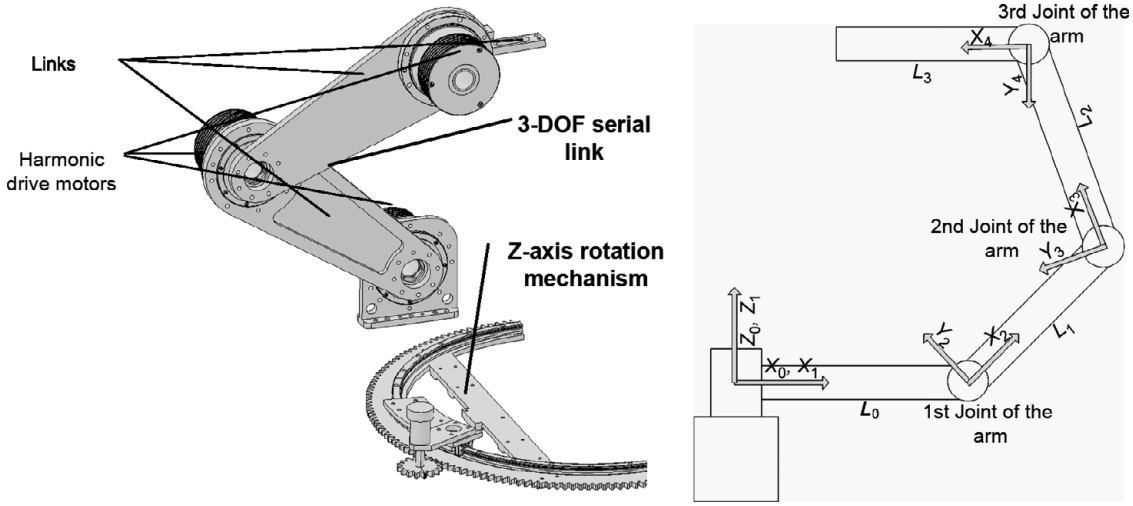

Fig. 8. The 4-DOF climbing mechanism of the 3DCLIMBER.

https://doi.org/10.1017/S0263574710000676 Published online by Cambridge University Press

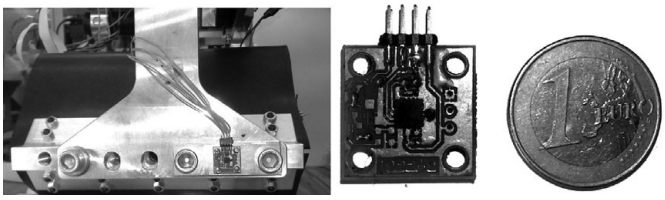

Fig. 9. The inclinometer board installed on one of the grippers.

Table I. Mean value of the V_{out} of "Y" axis with existence of vibrations of various amplitudes and frequencies.

Mean value of the V_{out} of "Y" axis	1.21745 V
Mean value of the V_{out} of "Y" axis with 6-Hz vibration	1.21751 V
Mean value of the V_{out} of "Y" axis with 3-Hz vibration	1.21757 V
Mean value of the V_{out} of "Y" axis with 5-Hz wider amplitude vibration (compared to both previous experiments)	1.21839 V

Table II. Characteristics of inclinometer sensors developed with the STM LIS244AL 2 axes accelerometer chip.

Sensitivity	From 3 mV° to 6 mV°
Repeatability based on one sample	4°
Repeatability based on average of 400 samples at 100 Hz	0.07°
Repeatability based on average of 400 samples at 100 Hz and existence of 5-Hz mechanical vibrations	0.2°

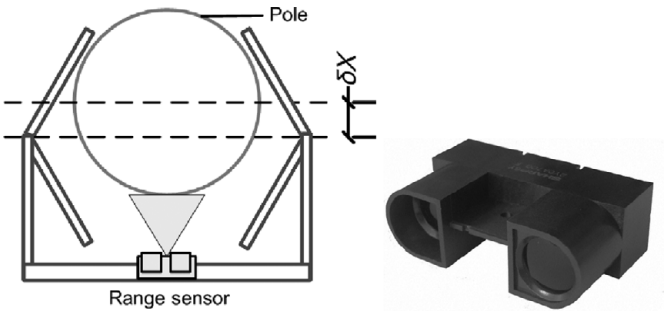

Fig. 10. Schematic of the gripper distance error compensation.

sensors (Fig. 10). These sensors can measure distances in the range of 10 to 80 cm. These sensors are based on geometrical principals, being highly independent of the optical properties of the target surface.

As the 4-DOF mechanism does not include the translation along the "Y" axis, the infrared sensors were not utilized. Consequently, for the 3DCLIMBER, the self-calibration algorithm can be achieved only with low-cost range-finders and accelerometers. Two range-finders are installed on each gripper. One of them is necessary to measure the distance between the gripper and the part of the structure that the robot is climbing from and the other is for correctly positioning the manipulator below the bent section, before traversing to the

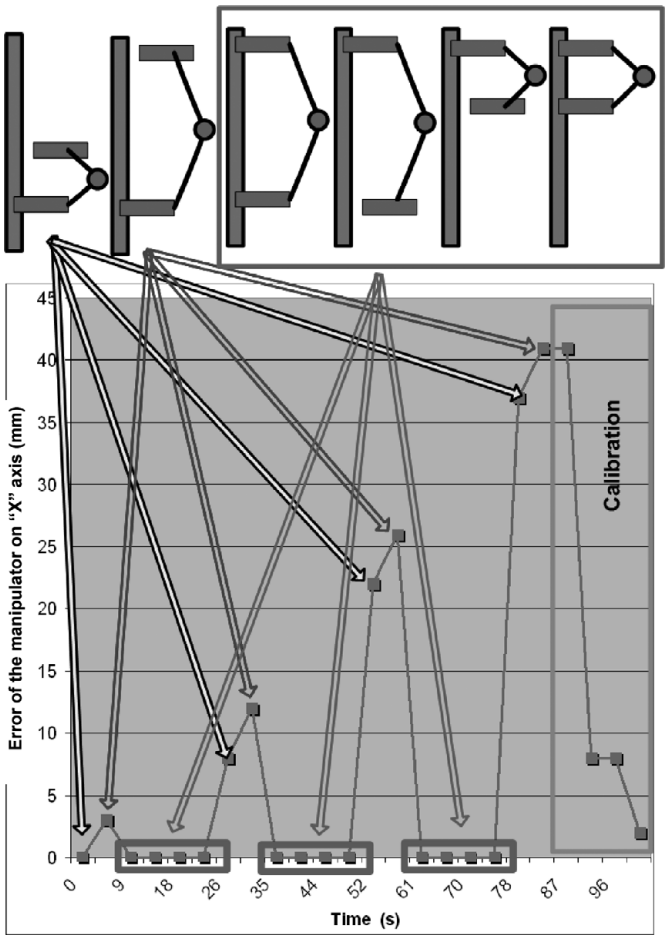

Fig. 11. Error in X direction against time, for execution of three sequential straight line steps followed by the self-calibration algorithm. This chart demonstrates the error measured on the upper gripper, which is not the total error of the system.

bent section. The total cost of the sensors embedded in the 3DCLIMBER is less than US$ 100.

4.2. Results

By integrating the above-mentioned sensors, and using the simplified version of the algorithm as shown in Fig. 5, the positioning error of the system was reduced from 48 mm to 6 mm (both values in the worst case and in the X direction). The positioning error of the system based on the average of error in five straight climbing steps and in the X direction was reduced from 12 mm to 2.5 mm, provided that the self-calibration algorithm runs after the execution of each step (each step of the 3DCLIMBER is defined as follows: upper gripper moves one step up, upper gripper grasps the structure, lower gripper opens, goes one step up and grasps the structure, and finally the upper gripper opens). Application of the more precise IMS and range sensors would improve the positioning error.

4.3. The first experiment

According to the accuracy requirements of the 3DCLIMBER, the system parameters are defined in a way that after three to six climbing steps, the positioning error of one of the components exceeds the predetermined allowed error and the self-calibration algorithm calibrates the system. Figure 11 shows the value of error in the X

https://doi.org/10.1017/S0263574710000676 Published online by Cambridge University Press

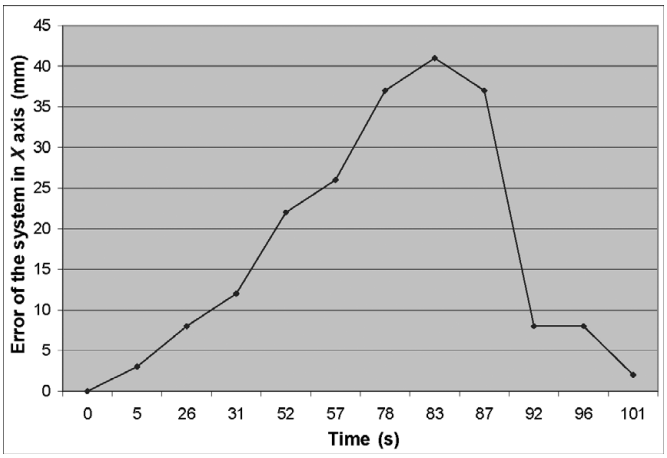

Fig. 12. Error in X direction against time, for execution of three sequential straight line steps followed by the self-calibration algorithm (zero values neglected).

direction against time for execution of three sequential straight line steps followed by the self-calibration algorithm. After the error on "X" axis exceeds a predetermined value, the accelerometer installed on the base of the robot (in this case the lower gripper) reports the deviation angle of the base for both axes (indicated as "C1" in Fig. 11), then all components of the error on the manipulator initiated from the base positioning error are compensated (indicated as "C2"). The third calibration step is to measure the error on the manipulator directly from the accelerometer and range finder installed on the manipulator (indicated as "C3"), and the final step is to compensate this error (C4). The maximum allowable error on "X" axis before the calibration algorithm starts was set equal to 40 mm. Of course, any value lower than 40 mm can also be used, but in this case the self-calibration algorithm will run more frequently than its current status.

The values in Fig. 11 show the error on the upper gripper and not the total error of the system. Every time the upper gripper grasps the structure, due to the special V-shaped design of the gripper, which has a self-centering characteristics, the ε_x of the upper gripper becomes zero temporarily. As the system forces this error to zero, it becomes "over defined," the links of the arm deflect, and consequently the climbing mechanism motors pull maximum current to compensate the error. When the error increases, the motors' current increases as well. For this reason in the chart presented in Fig. 11, when the error is shown equal to zero, it does not mean that the error of the system is zero, but shows that the system is over-defined. Figure 12 shows the same chart, after eliminating "zero" values.

A problem regarding the self-calibration algorithm is that it reduces the overall climbing speed, as it has to be applied after the execution of every few steps. To resolve this problem, the calibration algorithm is integrated in a climbing step. As shown in Fig. 5, the upper gripper moves one step up, but before gripping the structure, the calibration algorithm moves the upper gripper to a more accurate gripping position. Similarly the lower gripper will be calibrated in the same climbing step.

Table III shows some of the improvements on the robot performance after integration of self-calibration algorithms and sensors.

4.4. The second experiment

Another experiment was performed to test the self-calibration algorithm on bent sections. In this experiment the path includes one straight step, passing a 45° bent section (which can be done in two steps) and another straight step on the bent section. In this case the bent angle is provided to the path planner program. To extract the statistical distribution of the error, 10 identical experiments were performed. The other difference between this experiment and the previous one is that the maximum allowable error on "X" axis, which is the threshold value for the execution of the calibration algorithm, was set to 30 mm rather than 40 mm. The reason is that, according to the experiments when the robot is passing a bent section, bigger errors accumulate at each step compared to the time that it is only climbing a vertical straight structure. Therefore, as the safety tolerance from the maximum permissible error in "X" axis, which still assures safe gripping (=50 mm), should not be over-passed at any step, the threshold value that activates the self-calibration algorithm was reduced. Among the 10 experiments, in eight cases the self-calibration algorithm was executed after the third climbing step, and in the other two cases it was executed after the fourth step. Figure 13 shows the average value of the errors measured on "X" axis for all steps of the experiments and also their deviation from the mean value (the fourth climbing step and the calibration step are not shown in the figure).

4.5. The third experiment – type C errors

The third experiment was performed in order to test the proposed algorithm for compensation of the type C errors. In the case of 3DCLIMBER, the geometry of the structure should be provided to the robot by the operator. In this case, the robot was fixed and calibrated in a 45° bent section. The mission of the robot was defined as descending from the bent section to the vertical pole. However, the bent angle was provided as 55° rather than 45°. Figure 14 shows the result

Table III. Improvements on the robot's performance after integration of self-calibration algorithms and sensors.

Item	Before integration	After integration
Angular positioning error of grippers	1°–8°	1°
Positioning error type	Accumulative	Reset at each step
Positioning error in X direction in the worst case (maximum stroke while passing 45° bent section)	48 mm	6 mm
Positioning error in X direction: average of error in five straight climbing steps	12 mm	2.5 mm
Maximum permissible error in "X" axis, which still assures a safe gripping	50 mm	50 mm

https://doi.org/10.1017/S0263574710000676 Published online by Cambridge University Press

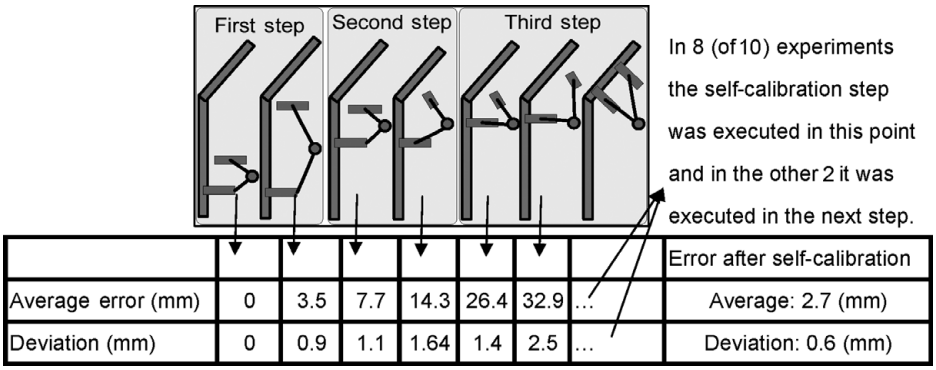

	↓	↓	↓	↓	↓	↓		Error after self-calibration
Average error (mm)	0	3.5	7.7	14.3	26.4	32.9	…	Average: 2.7 (mm)
Deviation (mm)	0	0.9	1.1	1.64	1.4	2.5	…	Deviation: 0.6 (mm)

Fig. 13. The average value of the errors measured on "X" axis for three climbing steps and also their deviation from the mean value for 10 identical experiments. In this figure only those parts of each step in which the upper gripper is open are demonstrated.

of this experiment. The lower gripper of the robot moves in a straight line base at 55° angle and the sharp range sensor measures the distance between the gripper and the structure, calculates the correct bent angle, and repositions the lower gripper to a correct position.

5. Conclusion and Outlook to Future Works

Mobile robots are usually equipped with an arm, which in some cases should perform activities that require high positioning accuracy. As the base of the arm is mobile, the manipulator of arm cannot take advantage of a fixed coordinate system, and thus contains positioning errors. In this paper, we addressed this problem by the integration of a self-calibration system. The system is not dependent on any external observer or transceiver as reference point. Using this system, the robot may calibrate itself several times during achievement of a specific mission. This system was implemented in a pole climbing robot and effectively improved its positioning accuracy.

Sensors used in this study were low-cost accelerometers and IR range sensors. As the efficiency of the proposed system was proved in the experiments, more applications for the proposed system might be considered. Also, alternative approaches for the compensation of the introduced errors can be investigated. For instance, to compensate for the type B errors, an alternative approach to the proposed repeated self-calibration might be to include a closed loop continuous compensation of the error on the online path-tracking algorithm. In the most general form, three range sensors on each plane can continuously measure the distance to the adjacent environment, and adjust the angle and distance of the adhesion zone to the environment. A 2D representation of the approach with two range sensors is demonstrated in Fig. 15.

The integration of sensors, error compensation algorithms, and calibration algorithms to the climbing robots is vital for most of the testing and maintenance applications. Even though many solutions for the climbing and gripping mechanisms of climbing robots have been proposed during the last two decades, sensor integration and automation of these robots were mostly neglected. This is probably one of the reasons that climbing robots are not being widely used in industrial applications. This paper is a step toward automation of climbing robots and enhancement of the manipulation accuracy. Regarding the gripping problems because of positioning error, there might exist other solutions, such as application of compliant materials and mechanisms, or compliant control, so that the gripping action might be possible in case of the existence of positioning errors on the gripper. Yet, integration of compliance in the gripper not only compensates the type B error on the manipulator but also increases the difference between the real position and the estimated position of the gripper. Therefore, sensors are necessary to measure errors on the gripper position. In fact, compliant mechanism solutions can be combined by the

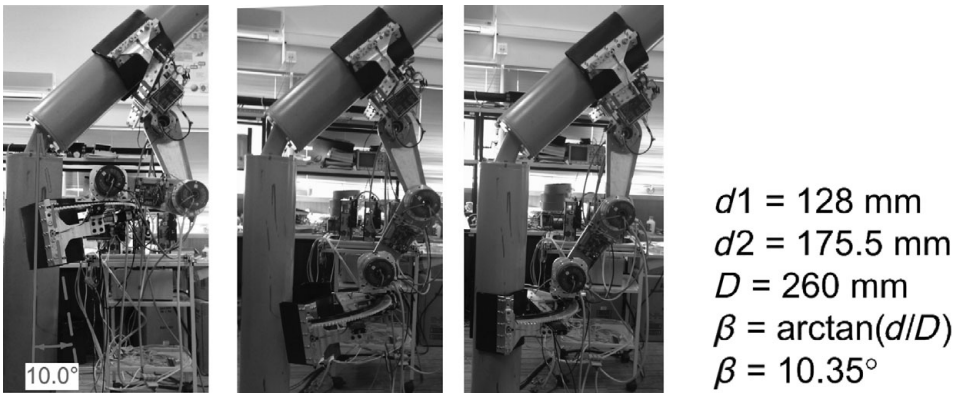

Fig. 14. Running the type C error compensation algorithm, the correct bent angle is calculated and the lower gripper is placed in the correct position. Parameters are defined in Fig. 6.

https://doi.org/10.1017/S0263574710000676 Published online by Cambridge University Press

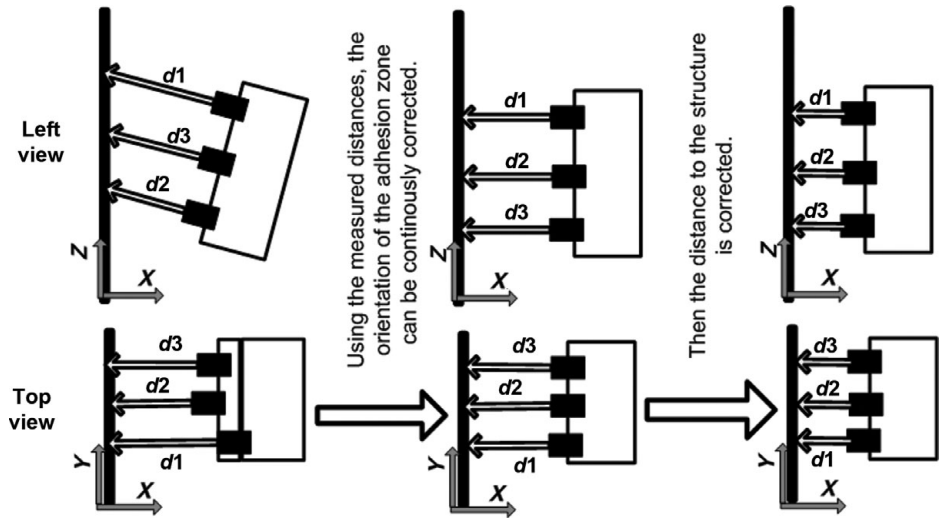

Fig. 15. A continuous control loop that receives measurements from three range sensors is an alternative approach for compensation of type B errors.

proposed method in this paper in order to establish a good trade off between the compliance and tolerance to the error on the gripper and positioning accuracy on the manipulator.

References

1. R. Aracil, R. Saltarén and O. Reinoso, "Parallel robots for autonomous climbing along tubular structures," *Robot. Auton. Syst.* **42**(2), 125–134 (2003).
2. C. Balaguer, A. Gimenez and C. Abderrahim, "ROMA robots for inspection of steel-based infrastructures," *Ind. Robot. Int. J.* **29**(3), 246–251 (2002).
3. C. Balaguer, A. Giménez, J. Pastor, V. Padrón and M. Abderrahim, "A climbing autonomous robot for inspection applications in 3D complex environments," *Robotica* **18**(03), 287–297 (2000).
4. C. Balaguer, J. Pastor, A. Giménez, V. Padrón and M. Abderrahim, "Roma: A Multifunctional Autonomous Self-Supported Climbing Robot for Inspection Application," *3rd IFAC Symposium on Intelligent Autonomous Vehicles*, Madrid, Spain (1998) pp. 357–362.
5. P. Borgstrom, B. Jordan, B. Borgstrom, M. Stealey, G. Sukhatme, M. Batalin and W. Kaiser, "Nims-pl: A cable-driven robot with self-calibration capabilities," *IEEE Trans. Robot.* **25**(5), 1005–1015 (2009).
6. J. Cannon, H. Robert and E. Schmitz, "Initial experiments on the end-point control of a flexible one-link robot," *Int. J. Robot. Res.* **3**(3), 62 (1984).
7. J. Craig, *Introduction to Robotics: Mechanics and Control* (Addison-Wesley Longman, Boston, MA, 1989).
8. W. Fischer, F. Tache, G. Caprari and R. Siegwart, "Magnetic Wheeled Robot with High Mobility but only 2 DOF to Control," *Proceedings of The 11th International Conference on Climbing and Walking Robots and the Support Technologies for Mobile Machines (CLAWAR)*, Coimbra, Portugal (2008).
9. A. Goswami, A. Quaid and M. Peshkin, "Complete Parameter Identification of a Robot from Partial Pose Information," *IEEE International Conference on Robotics and Automation*, Citeseer, Atlanta, GA, USA (May 2–6, 1993), pp. 168–168.
10. W. Khalil and S. Besnard, "Self calibration of Stewart-Gough parallel robots without extra sensors," *IEEE Trans. Robot. Autom.* **15**(6), 1116–1121 (1999).
11. J. Lin and F. Lewis, "Two-time scale fuzzy logic controller of flexible link robot arm," *Fuzzy Sets Syst.* **139**(1), 125–149 (2003).
12. H. H. S. Liu and G. Pang, "Accelerometer for mobile robot positioning," *IEEE Trans. Indus. Appl.* **37**(3), 812–819 (2001).
13. D. Longo and G. Muscato, "The Alicia3 climbing robot," *IEEE Robot. Autom. Mag.* **13**(1), 42 (2006).
14. M. Meggiolaro, S. Dubowsky and C. Mavroidis, "Error identification and compensation in large manipulators with application in cancer proton therapy," *Revista Brasileira de Controle & Automaç ao* **15**(1), 71–77 (2004).
15. M. Meggiolaro, P. Jaffe and S. Dubowsky, "Achieving Fine Absolute Positioning Accuracy in Large Powerful Manipulators," *Proceedings of IEEE International Conference on Robotics and Automation*, Detroit, Michigan, USA (1999).
16. C. Menon, M. Murphy and M. Sitti, "Gecko Inspired Surface Climbing Robots," *IEEE International Conference on Robotics and Biomimetics (ROBIO)*, Shenyang, China (2004) pp. 431–436.
17. M. Rachkov, L. Marques and A. de Almeida, "Climbing Robot for Porous and Rough Surfaces," **In**: *5th International Conference on Climbing and Walking Robots and the Support Technologies for Mobile Machines* (P. Bidaud and F. B. Amar, eds.) (Professional Eng. Pub., 2002).
18. A. Rauf and J. Ryu, "Fully Autonomous Calibration of Parallel Manipulators by Imposing Position Constraint," **In**: *IEEE International Conference on Robotics and Automation*, vol. 3 (2001) pp. 2389–2394.
19. M. Tavakoli, A. Marjovi, L. Marques and A. de Almeida, "3DCLIMBER: A Climbing Robot for Inspection of 3D Human Made Structures," *IEEE/RSJ International Conference on Intelligent Robots and Systems, IROS*, Nice, France (2008) pp. 4130–4135.
20. M. Tavakoli, L. Marques and A. T. de Almeida, "Self-Calibration of Step-by-Step Based Climbing Robots," *IROS*, St. Louis, MO (2009) pp. 3297–3303.
21. M. Tavakoli, M. Zakerzadeh, G. Vossoughi and S. Bagheri, "Design and Prototyping of a Hybrid Pole Climbing and Manipulating Robot with Minimum DOFs for Construction and Service Applications," *Climbing and Walking Robots: Proceedings of the 7th International Conference (Clawar 2004)*, Madrid, Spain (2004).
22. M. Tavakoli, M. Zakerzadeh, G. Vossoughi and S. Bagheri, "A hybrid pole climbing and manipulating robot with minimum DOFs for construction and service applications," *J. Indus. Robot.* **32**(2), 171–178 (2005).
23. M. Tavakoli, M. Zakerzadeh, G. Vossoughi, S. Bagheri and H. Salarieh, "A Novel Serial/Parallel Pole Climbing/Manipulating Robot: Design, Kinematic Analysis and Workspace Optimization with Genetic Algorithm," *21th International Symposium on Automation and Robotics in Construction*, Jeju Island, Korea (2004).

https://doi.org/10.1017/S0263574710000676 Published online by Cambridge University Press